Corneodesmosin gene ablation induces lethal skin-barrier disruption and hair-follicle degeneration related to desmosome dysfunction

Emilie A. Leclerc[1], Anne Huchenq[1], Nicolas R. Mattiuzzo[1], Daniel Metzger[2], Pierre Chambon[2], Norbert B. Ghyselinck[2], Guy Serre[1,*], Nathalie Jonca[1,‡] and Marina Guerrin[1,‡]

[1]UMR 5165 'Différenciation Epidermique et Autoimmunité Rhumatoïde' (UDEAR), CNRS – Université Toulouse III, IFR150, INSERM, CHU PURPAN, Place du Dr Baylac, TSA 40031, F-31059 Toulouse, Cedex 9, France
[2]IGBMC (Institut de Génétique et de Biologie Moléculaire et Cellulaire), Inserm U596 – CNRS UMR 7104 – Université Louis Pasteur – Collège de France, Illkirch, F-67400 France

*Author for correspondence (e-mail: Guy.Serre@udear.cnrs.fr)
‡These authors contributed equally to this work

Accepted 1 May 2009
Journal of Cell Science 122, 2699-2709 Published by The Company of Biologists 2009
doi:10.1242/jcs.050302

Summary

Corneodesmosin (CDSN) is specific to desmosomes of epithelia undergoing cornification, mainly the epidermis and the inner root sheath of the hair follicles. *CDSN* nonsense mutations are associated with hypotrichosis simplex of the scalp, a rare disease that leads to complete baldness in young adults. CDSN displays adhesive properties, mostly attributable to its N-terminal glycine-rich domain, and is sequentially proteolyzed as corneocytes migrate towards the skin surface. *K14*-promoter driven Cre-mediated deletion of *Cdsn* in mice resulted in neonatal death as a result of epidermal tearing upon minor mechanical stress. Ultrastructural analyses revealed a desmosomal break at the interface between the living and cornified layers. After grafting onto nude mice, knockout skin showed a chronic defect in the epidermal permeability barrier. The epidermis was first hyperproliferative with a thick cornified layer, then, both the epidermis and the hair follicles degenerated. In adults, *Cdsn* deletion resulted in similar histological abnormalities and in a lethal barrier defect. We demonstrate that *Cdsn* is not essential for skin-barrier formation in utero, but is vital throughout life to preserve this barrier by maintaining desmosome integrity. The strong adhesive function that the protein confers on corneodesmosomes also seems necessary for maintaining the architecture of the hair follicle.

Supplementary material available online at
http://jcs.biologists.org/cgi/content/full/122/15/2699/DC1

Key words: Desmosome, Epidermis, Hypotrichosis simplex of the scalp, Knockout mice, Psoriasis

Introduction

Lessons from human diseases and engineered mouse models have established the importance of desmosomes in tissues subjected to high mechanical stress. Indeed, these intercellular junctions provide strong cohesion between adjacent cells. Mutations in genes encoding desmosomal components are invariably responsible for skin diseases, often associated with heart defects (for reviews, see Kottke et al., 2006; Garrod and Chidgey, 2008). In the epidermis, desmosomes undergo profound morphological and biochemical changes throughout keratinocyte differentiation. In particular, during cornification, a specific cell death process that transforms keratinocytes into anucleated, flattened corneocytes, considerable modifications of the desmosomes occur, accounting for their designation as corneodesmosomes (Serre et al., 1991).

Corneodesmosin (CDSN) is a protein specific to desmosomes that will undergo transformation into corneodesmosomes, which, in humans, comprises desmosomes of the epidermis, the three layers of the inner root sheath (IRS) of the hair follicles and the hard palate epithelium. Indeed, the protein is not expressed in noncornified squamous epithelia (Serre et al., 1991). After its secretion by granular keratinocytes via the lamellar granules, CDSN is incorporated into the desmoglea of the desmosomes shortly before their transformation into corneodesmosomes, most probably reinforcing the cell-cell adhesion mediated by the desmosomal cadherins already present in the structure. In the course of stratum corneum maturation, CDSN is progressively degraded, its degradation being a prerequisite for desquamation (Simon et al., 2001).

Cloning of its cDNA has revealed that *CDSN* is located on chromosome 6, in the major psoriasis susceptibility locus PSORS1 (Guerrin et al., 1998). Some *CDSN* single nucleotide polymorphisms (SNPs) have been associated with psoriasis in many genetic studies (reviewed by Capon et al., 2002), and a recent study revealed that only two genes from PSORS1, *HLAC* and *CDSN*, yield protein alleles that are unique to risk haplotypes (Nair et al., 2006). However, according to the latter study and others, the exact identity of the PSORS1 gene remains controversial (Veal et al., 2002; Capon et al., 2003; Helms et al., 2005; Orrù et al., 2005; Nair et al., 2006). Intriguingly, the only monogenic disease identified so far to be associated with mutations in *CDSN* revealed a hair phenotype and did not affect the epidermis (Levy-Nissenbaum et al., 2003); hypotrichosis simplex of the scalp (HSS; OMIM 146520) is a rare autosomal-dominant disease characterized by progressive loss of scalp hair resulting in almost complete baldness by the third decade.

To date, three different nonsense mutations have been reported in four families from Israel, Denmark and Mexico (Lai-Cheong et al., 2007). These mutations lead to the production of a truncated form of CDSN that has been detected as deposits beneath the epidermis basement membrane and deeper in the dermis, at the periphery of the hair follicles (Levy-Nissenbaum et al., 2003). Although the pathophysiological mechanism of this disorder is not understood, CDSN obviously has an important role in hair physiology.

A striking feature of CDSN is its very high serine and glycine content (27.5% and 16%, respectively), particularly at the N-terminus of the protein (residues 60-171). It has been suggested that similar serine- and glycine-rich domains described at both termini of keratins form structural motifs, the so-called 'glycine loops', that mediate intermolecular adhesion by acting like Velcro (Steinert et al., 1991). Furthermore, it has been demonstrated, in vivo and in vitro, that CDSN displays homophilic adhesive properties (Jonca et al., 2002; Caubet et al., 2004). Moreover, recombinant CDSN forms highly stable homo-oligomers that dissociate only partially in 8 M urea, possibly reflecting *cis* and/or *trans* interactions in vivo. The N-terminal glycine loop domain was shown to be necessary and sufficient, and thus responsible, for both the oligomerization of CDSN and its homophilic adhesive properties in vitro (Caubet et al., 2004).

In vivo, CDSN could thus mediate cell-cell adhesion by reinforcing the resistance of the desmosomes. It has also been proposed that CDSN contributes to the structural modifications that characterize the transformation of desmosomes into corneodesmosomes (Guerrin et al., 1998) or prevents premature desquamation by protecting desmosomal proteins from proteolysis (Lundström et al., 1994). Inactivation of mouse *Cdsn* by mutational insertion was very recently reported to induce neonatal death (Matsumoto et al., 2008), and defective corneodesmosome formation was proposed to be responsible for stratum corneum detachment.

We developed two epidermal-selective *Cdsn*-deficient mouse models. Somatic *Cdsn* inactivation in mouse epidermis was achieved using human keratin 14 (*K14*)-promoter driven Cre-mediated deletion (Li et al., 2001). Temporally controlled *Cdsn* deletion in epidermal keratinocytes was achieved using a tamoxifen-inducible Cre recombinase under the control of the same promoter (Li et al., 2000). Our results confirmed the vital role of CDSN in newborns. We also show that CDSN function is essential in adult skin and that the functional defect lies in an impaired resistance of corneodesmosomes to mechanical stress. This supports the idea that CDSN mainly acts as an adhesive protein.

Results

Generation of *Cdsn*-deficient mice

To investigate the role of CDSN in the barrier function and physiology of the hair follicle, we developed *Cdsn*-deficient mice by using *K14*-promoter driven Cre-mediated *lox*P recombination (Fig. 1A). The human *KRT14* promoter is active during mouse epidermal fetal development as early as embryonic day (E)9.5, and is strongly activated by E14.5 onwards (Vassar et al., 1989). Similarly to many other markers of epidermis differentiation, *Cdsn* mRNA was first detected at E16.5 and becomes prominent at E18.5 (H.G., unpublished results). Therefore, the chosen strategy would induce the deletion of the second exon of *Cdsn* before the gene is expressed in the developing epidermis and in hair follicles.

We first generated mice bearing floxed *Cdsn* alleles ($Cdsn^{fl/fl}$), which were bred to homozygosity. These animals appeared normal, indicating that the genetic manipulation did not affect the function of the floxed gene. Generation of *Cdsn*-deficient mice was obtained by crossing $Cdsn^{fl/fl}$ mice with *K14-Cre* transgenic mice (Li et al., 2001). The resulting animals bearing the *K14-Cre* and heterozygous for the floxed *Cdsn* allele were selected and mated again with $Cdsn^{fl/fl}$ mice. Four different genotypes were thus obtained (Fig. 1B): $K14\text{-}Cre^{0/0}$:$Cdsn^{wt/fl}$ and $K14\text{-}Cre^{0/0}$:$Cdsn^{fl/fl}$, both denoted hereafter as wild-type (WT), $K14\text{-}Cre^{tg/0}$:$Cdsn^{wt/fl}$, denoted hereafter

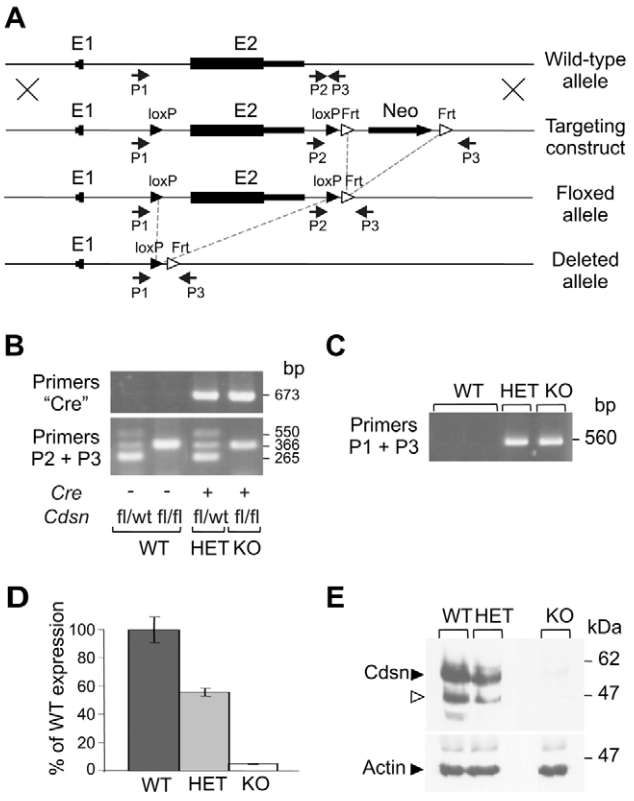

Fig. 1. Gene targeting of *Cdsn*. (A) Schematic drawing of the *Cdsn* wild-type locus, the targeting construct (containing the neomycin selector gene), the floxed allele, and the deleted allele obtained after Cre-mediated excision. The floxed part of *Cdsn* (3 kb) encompasses the second exon, so only the first exon, which encodes 28 amino-acids mostly corresponding to the signal peptide, is preserved after Cre-mediated recombination. Black boxes represent exons, *loxP* and Frt sites are depicted as black and open triangles, respectively. Primers for PCR genotyping (P1-P3) are indicated with arrows. (B) PCR analysis of tail DNA from offspring of $Cdsn^{fl/fl}$ mice crossed with $K14\text{-}Cre^{tg/0}$:$Cdsn^{fl/wt}$ (HET) mice. Specific primers were used to detect the *K14-Cre* transgene (primers 'Cre'). Primers P2 and P3 were used to detect wild-type (265 bp) or floxed (366 bp) *Cdsn* alleles. A 550 bp band was detected only in heterozygous pups, which corresponds to the amplification of partial hybridization between 265 bp and 366 bp amplicons, as verified by sequencing. (C) Primers P1 and P3 allow the amplification of a 560 bp fragment when the exon 2 of *Cdsn* is excised. The experimental conditions used for this PCR do not allow amplification of the non-excised 3.7 kb fragment still containing the second exon. (D) Quantitative RT-PCR analysis of *Cdsn* expression on dorsal skin samples from WT, HET and KO neonates. Values represent relative RNA level from the WT, after normalization with *Dsg3* transcript level. Values are mean ± s.e.m. (E) Equal amounts of protein extracts from WT, HET and KO neonate dorsal skin were separated by SDS-PAGE and subjected to western blot analysis using the anti-CDSN F28-27 mAb or an anti-actin mAb. In protein extracts from WT and HET animals, F28-27 reacts with two major polypeptides of about 54 kDa and 45 kDa, which correspond to the full-length (black triangle) and a proteolytically processed form of CDSN (open triangle), respectively.

as heterozygous mice (HET), and *K14-Cre*$^{tg/0}$:*Cdsn*$^{fl/fl}$, denoted as knockout (KO) mice. The genotyping of 232 newborns from 12 intercrosses revealed that WT, HET and KO pups were produced in the expected mendelian ratios, indicating no embryonic lethality for the KO mice. Excision of the floxed *Cdsn* allele in the skin of newborn pups was controlled by PCR analysis (Fig. 1C). As expected, in skin of KO neonates, *Cdsn* mRNA level measured by quantitative real-time PCR was very low, confirming efficient ablation of *Cdsn* (Fig. 1D). In HET pup skin, *Cdsn* expression was roughly 50% of the WT level, demonstrating the absence of dose compensation. Western blot analysis (Fig. 1E) using the F28-27 anti-CDSN monoclonal antibody (mAb) confirmed the absence of CDSN in the skin of KO animals, whereas the full-length 54 kDa protein was detected in skin extracts from WT and HET animals. The smaller amount of protein in HET mice is consistent with results of RT-PCR analysis, which indicate inactivation of one *Cdsn* allele. A lower molecular mass peptide of ~45 kDa was also detected in both WT and HET pup extracts, which corresponds to a first step of the CDSN proteolytic cleavage in the course of stratum corneum maturation (Simon et al., 1997).

Inactivation of CDSN in mouse skin results in early postnatal death

KO pups suffered from severe skin detachment (Fig. 2A) and died within 1 hour of birth or were immediately eliminated by their mother. To delineate the causes of neonatal lethality, we systematically performed caesarian deliveries at E18.5. Under these conditions, KO embryos were indistinguishable from their littermates when handled carefully (Fig. 2B). However, during grooming by surrogate mothers we observed the rapid appearance of skin detachment that was similar to that observed after natural birth. Skin rupture started in the ventral area, paws and snout and extended to the flanks (Fig. 2C). The peeled skin was red, shiny, and became somewhat sticky to the touch. On the dorsal part of the pups, the skin retained a normal macroscopic aspect until death, which occurred within 2 hours. A standard procedure for analysis of the phenotype was thus established: after caesarian delivery, all neonates were given to a surrogate mother and euthanized after 1 hour.

Inactivation of CDSN in mouse skin leads to a drastic barrier defect

To measure the effects of the mutation on skin permeability, we performed a Toluidine blue penetration assay on E18.5 embryos (Fig. 3A). When the assessment was carried out immediately after caesarian delivery, before any skin phenotype onset, complete dye exclusion was observed in KO pups, as in their control littermates, reflecting an intact barrier at that stage (Fig. 3A, left panels). However, when mice were given to a surrogate mother for 1 hour, large areas showed toluidine blue penetration, particularly in the ventral part of the embryos (Fig. 3A, right panels). Thus, as soon as a skin phenotype became macroscopically visible in KO animals, the dye extensively penetrated the skin. This drastic perturbation of the barrier could be perfectly superimposed with the zones of detachment of the stratum corneum in KO animals (see Fig. 2C). Similarly, transepidermal water loss (TEWL) measured on whole pups was similar at first in WT, HET and KO pups immediately after caesarian delivery but dramatically increased by a factor greater than ten in KO mice after phenotype onset (Fig. 3B). To maintain conditions of minimal mechanical stress, KO neonates were isolated at 37°C for 4 hours, immediately after caesarian section. Under these conditions, only one out of nine KO pups died. The remaining pups did not develop any noteworthy skin detachment, and five of them maintained a TEWL value that was roughly similar to that of the WT and HET newborns, between 0 and 4 g m^{-2} per hour. These experiments demonstrate that the skin phenotype is closely linked to mechanical stress from the environment. To assess the mechanical resistance of the skin, the amount of protein detached from the skin by tape stripping was measured. Three times more protein was extracted from KO skin than from WT or HET skin (Fig. 3C). Hence, even macroscopically intact KO skin is extremely fragile, and tears under mechanical stress.

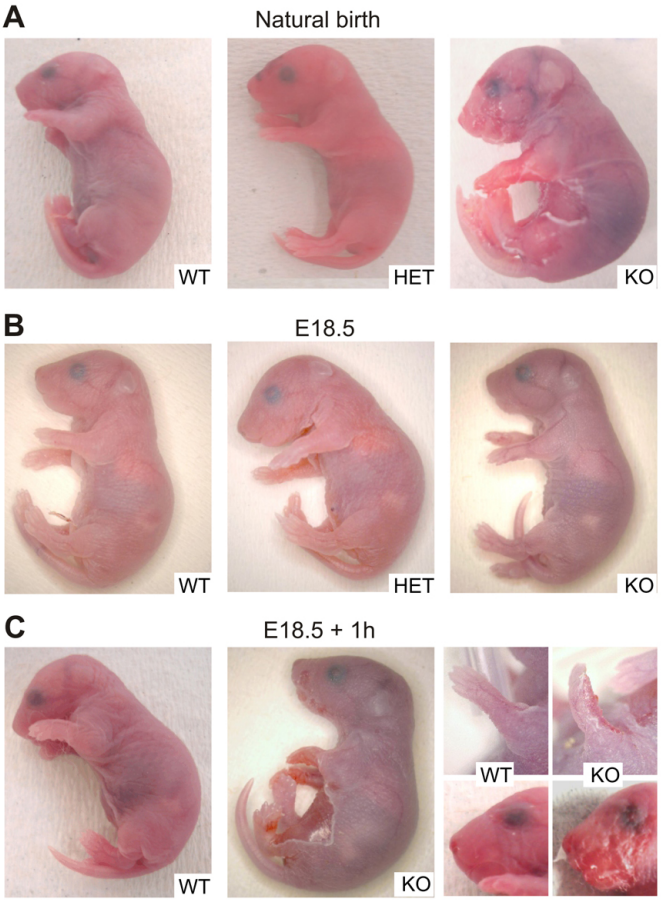

Fig. 2. Mice lacking CDSN show a drastic skin tear leading to postnatal death. (A) Macroscopic appearance of WT, HET and KO pups born at full term. KO pups die within 1 hour of birth and show considerable skin detachment, particularly in the ventral area, paws and snout, whereas HET newborns show no visible difference from WT. (B) Macroscopic appearance of WT, HET and KO mice delivered by caesarian section at E18.5. Immediately after birth, KO neonates are indistinguishable from the WT and HET littermates. (C) When neonates were left in surrogate mother's care for 1 hour, the skin phenotype of KO pups appears and death occurs rapidly. Higher magnifications of paw and snout of WT and KO neonates are shown on the right.

Histological analysis of KO mouse skin reveals a detachment of the stratum corneum from the living layers of epidermis

In zones of skin rupture, such as the ventral region, a complete absence of the stratum corneum was observed (Fig. 4A). In some areas, the skin abrasion was more pronounced and also concerned part of the living layers (data not shown). On the dorsal skin, the

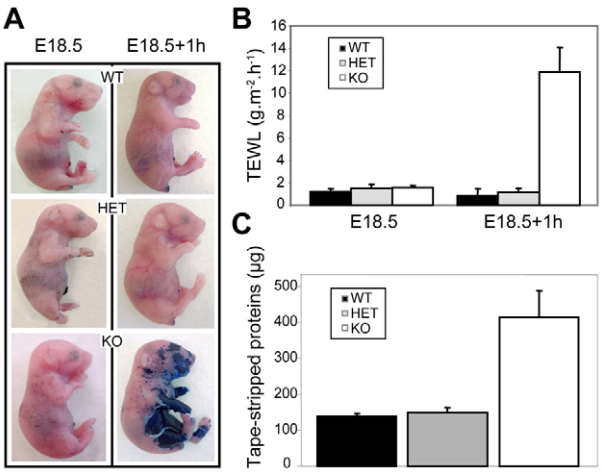

Fig. 3. Mice lacking CDSN exhibit a drastic barrier defect and decreased mechanical resistance of the skin. (A) Barrier-dependent dye exclusion assay (Toluidine blue) performed on WT, HET and KO neonates. Pups obtained by caesarian delivery (E18.5) were placed with surrogate mother for 1 hour until the skin phenotype appears (E18.5+1h). (B) TEWL assay performed on whole WT, HET or KO neonates immediately after caesarian delivery (E18.5) and after phenotype onset (E18.5+1h). (C) Mechanical resistance assay of the stratum corneum from neonates. Tape stripping was performed on the dorsal skin of WT, HET or KO neonates before phenotype onset, and the proteins present on the tape were quantified by colorimetric assay. Values are mean ± s.e.m.

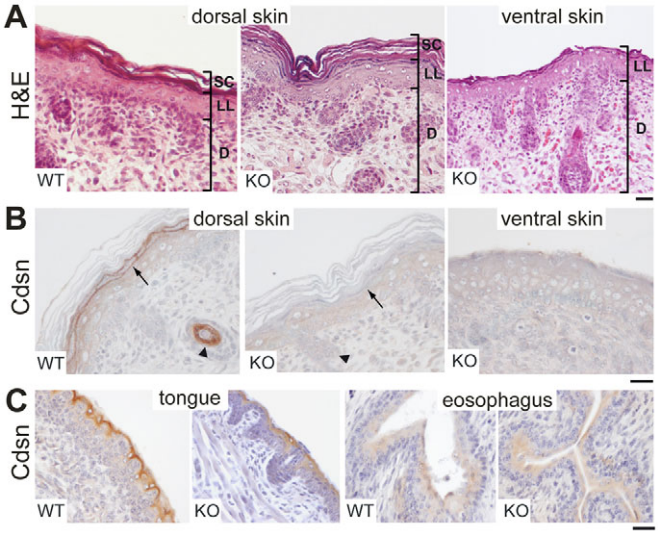

Fig. 4. Histological analysis of cornified epithelia in *Cdsn* KO mice. (A) Representative sections stained with hematoxylin and eosin (H&E), from dorsal skin of WT and KO neonates, or from ventral skin of KO neonates. The staining shows complete detachment of the SC from the ventral epidermis of the KO mouse. D, dermis; LL, living layers of epidermis; SC, cornified layer. (B) Immunohistochemical staining with F28-27 mAb (CDSN) of sections from dorsal skin of WT and KO neonates, or from ventral skin of KO neonates, confirmed the absence of CDSN in the stratum granulosum of the epidermis (arrows) and the IRS of the hair follicles (arrowheads) of KO pups. (C) Immunohistochemical staining with F28-27 mAb (CDSN) of sections from tongue and esophagus of WT and KO neonates showing that *Cdsn* excision is not efficient in internal epithelia. Scale bars: 20 µm.

stratum corneum was still present, and looked similar to that of the WT. However, even if the macroscopic aspect was normal, some blisters were observed between the stratum granulosum and stratum corneum (data not shown). Although we could not discriminate between blisters induced by natural mechanical stress or during sample preparation, our results suggest an extreme fragility of the intercellular links. No acanthosis or hyperkeratosis was observed in either dorsal or ventral KO epidermis. Immunohistochemical labeling of skin sections with F28-27 mAb confirmed the complete absence of CDSN in the stratum granulosum and IRS of hair follicles in KO mice (Fig. 4B). Transcriptional activity of the human *KRT14* promoter in transgenic mice is largely restricted to external epithelia, with a reduced expression in more internal stratified tissues (Wang et al., 1997). In accordance with these findings, CDSN was still detected in the tongue, the hard palate and the esophagus of KO newborns (Fig. 4C; and data not shown).

Corneodesmosomes deficient for CDSN display normal morphology but impaired functionality

Transmission electron microscopy performed on dorsal skin of WT and KO neonates revealed a similar organization of the granular layer. The thickness of stratum corneum from KO mice was also unchanged, with 10 to 13 layers (Fig. 5A,B). Some blisters, already detected by optical microscopy, were present between the stratum granulosum and stratum corneum (Fig. 5J; and data not shown). The ultrastructure of desmosomes and corneodesmosomes was analyzed at higher magnification. In granular keratinocytes from both WT and KO animals, the same characteristic symmetrical tri-lamellar structure of regular desmosomes was observed (Fig. 5C,F). Morphological changes accompanying cornification occurred similarly in both WT and KO mice. Typical transitional junctions were found, with classical dense fibrils of keratin filaments attached to the electron-dense intracellular desmosomal plaque in the granular keratinocyte, densification of the intercellular portion, and an electron-dense line at the other side of the junction corresponding to the cornified envelope of the upper transitional keratinocyte (Fig. 5D,G). The number of these transitional desmosomes at the interface between the stratum granulosum and stratum corneum was not significantly different in WT and KO samples. We made counts on 30 fields at magnification ×20,000, corresponding to the length of 3-4 corneocytes, and found 59 transitional desmosomes in the KO skin section versus 61 in the WT. Hence, in newborn KO mice, *Cdsn* deficiency seems to have no consequences on the transformation of desmosomes into corneodesmosomes. In the cornified layers, the morphology of the corneodesmosomes from KO mouse also appeared classical (Fig. 5E,H). By contrast, numerous split desmosomes could be observed at the transition from stratum granulosum to stratum corneum, either isolated (Fig. 5I) or adjacent in zones of detachment (Fig. 5J). The main structure of the split transitional desmosomes remained attached to the granular keratinocyte, and no cell lysis was observed. Desmosome breaking seemed to occur specifically at the stratum granulosum to stratum corneum transition, because no split corneodesmosomes were observed higher in the stratum corneum. Thus, abnormalities due to the absence of CDSN seem to occur only when cornification takes place, and lie in adhesive defects.

Absence of CDSN does not affect expression of differentiation markers and desmosomal proteins in neonatal epidermis

Histological analysis revealed no thickening of the living layers in the epidermis from KO neonate dorsal skin. To further investigate

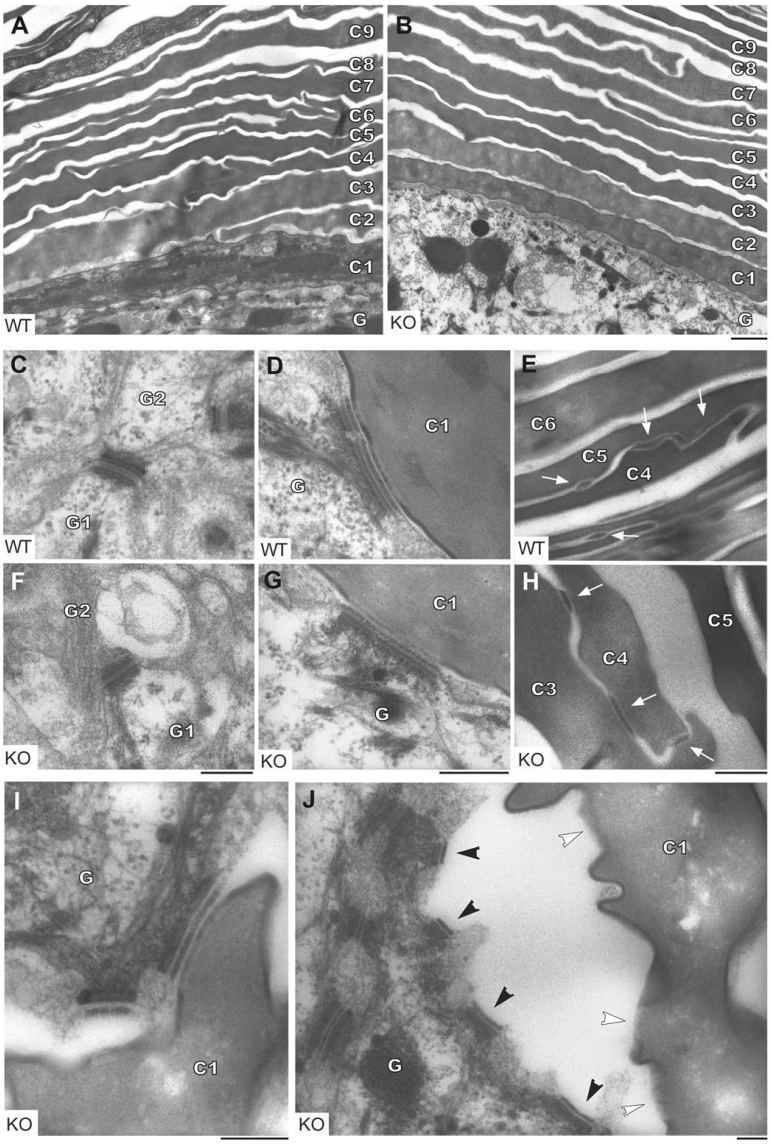

Fig. 5. Ultrastructural abnormalities in KO neonate epidermis. Dorsal skin of WT and KO mice was processed for transmission EM. (A,B) At low magnification, the cells at the junction between the granular and cornified layers have no obvious abnormality. G,G1,G2, granular keratinocytes; C1 to C9, corneocytes, with C1 being adjacent to the granular layer and C9 being nearest the skin surface. (C-H) The ultrastructure of desmosomes and corneodesmosomes from WT (C-E) and KO (F-H) epidermis analyzed at higher magnification. Regular desmosomes in the stratum granulosum (C,F), transitional desmosomes at the stratum granulosum to stratum corneum interface (D,G), and corneodesmosomes (white arrows) in the stratum corneum (E,H), show the same classical morphology in WT and KO epidermis. (I,J) Detachment between granular keratinocyte and corneocyte is frequently observed in KO epidermis. Split desmosomes isolated (I) or adjacent (J) can be seen. The mid-dense intercellular plugs of the detached transitional desmosomes remain associated with the granular keratinocyte (black arrowhead), whereas an interruption in the electron-dense line corresponding to the cornified envelope is clearly visible at the surface of the corneocyte, at the site where the desmosome was attached (white arrowhead). Scale bars: 2 µm (A,B), 0.2 µm (C-I).

the effect of the null mutation on epidermal differentiation, we examined the expression of differentiation markers and desmosomal proteins by western blot, quantitative real-time PCR and immunohistochemistry (Fig. 6). No significant differences in the amount of early (keratin K10, involucrin, desmoglein 1) and late (loricrin, filaggrin) differentiation markers were observed in skin from WT, HET or KO neonates by western blot analysis (Fig. 6A). Expression level analysis by qRT-PCR of *Dsc1*, *Dsg1a* and *Dsg1b*, coding for desmosomal proteins present in the suprabasal layers of epidermis, did not reveal any differences between the dorsal skin of WT and KO neonates (Fig. 6B). Immunohistochemical analyses (Fig. 6C) were consistent with the western blot and qRT-PCR data. Again, no differences in the distribution or the expression level of differentiation markers were observed between WT and KO neonate dorsal skin. As expected, we observed a dramatic reduction in the expression level of all the differentiation markers in the ventral area of KO animals (data not shown), which is consistent with the sudden loss of the most suprabasal keratinocytes once the stratum corneum had been shed (see Fig. 4A). In conclusion, the absence of CDSN does not affect the expression of differentiation markers and desmosomal proteins as long as the integrity of the epidermis is preserved.

Long-term phenotype of mouse skin lacking CDSN after grafting onto nude mice

The drastic barrier defect that occurs in KO mice does not allow the long-term consequences of *Cdsn* excision to be analyzed in the epidermis and hair follicle. To address this issue, full-thickness dorsal skin from WT and KO neonates was grafted onto the back of nude mice (Fig. 7). Absence of CDSN in the epidermis and IRS of hair follicles from KO grafts was controlled by immunohistochemistry (data not shown). Macroscopically, newborn KO skin developed some sparse hair that progressively disappeared and became totally absent 9 weeks after grafting. In parallel, the graft became hard, devoid of softness, and formed a scab that was continually renewed (Fig. 7A). In contrast to the WT, KO epidermis first showed a prominent hyperplasia with papillomatosis (Fig. 7B). Hyperkeratosis and parakeratosis were obvious and infiltration of inflammatory cells was observed in the dermis, together with dermal cysts, which characteristically result from degenerative hair follicles

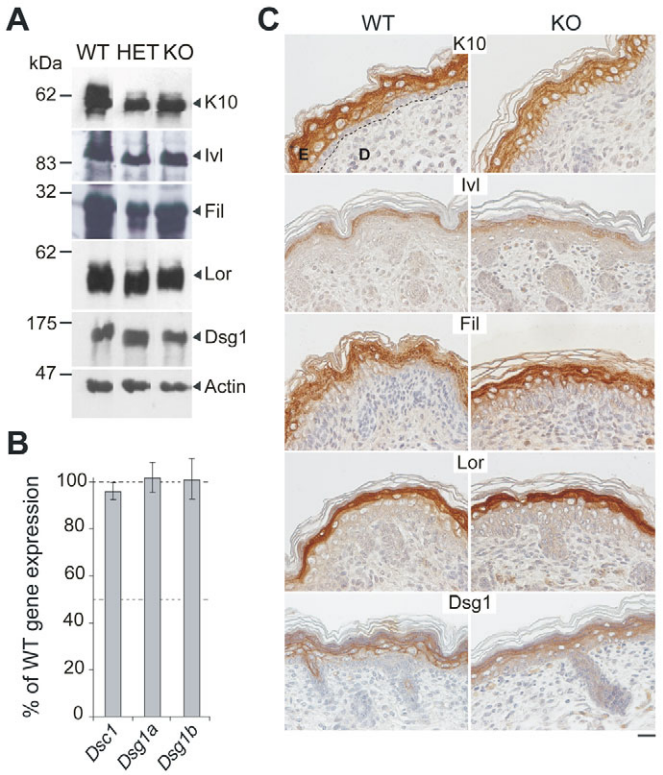

Fig. 6. Expression analysis of epidermal differentiation markers and desmosomal proteins in neonatal KO mice. (A) Equal amounts of protein extract from WT, HET and KO neonate dorsal skin separated by SDS-PAGE and analyzed by western blot with antibodies directed against keratin 10 (K10), involucrin (Ivl), filaggrin (Fil), loricrin (Lor), desmoglein 1 (Dsg1) or actin. (B) Quantitative RT-PCR analysis of genes encoding desmosomal proteins. *Dsc1*, *Dsg1a* and *Dsg1b* expression analyzed in dorsal skin biopsies from KO neonates. Values are shown relative to RNA level in the WT, after normalization with *Dsg3* transcripts, to take the epidermal area of each sample into account. Values are mean ± s.e.m. (C) Immunohistochemical labeling of dorsal skin sections from WT and KO neonates using antibodies specific to keratin 10 (K10), involucrin (Ivl), filaggrin (Fil), loricrin (Lor) and desmoglein 1 (Dsg1) shows a similar expression level and localization of the differentiation markers in WT and KO pups. D, dermis; E, epidermis; dotted line, dermoepidermal junction. Scale bar: 20 μm.

(Fig. 7D). Concomitantly, immunohistochemistry revealed high expression levels of keratin K6 and increased expression of several epidermal differentiation markers, such as involucrin, filaggrin, loricrin and K10 (Fig. 7C,E, left panel; and data not shown). From 8 weeks after grafting, despite its hyperproliferative state, the epidermis started to disappear in some central areas, replaced by a scab directly covering the dermis (Fig. 7B). By 9 weeks post grafting, this phenomenon had amplified, ending with the total absence of the grafted epidermis. In parallel, hair follicles became scarce and then totally disappeared. Concomitantly, the epidermis of the nude mice located at the edge of the initial graft became thicker, producing keratinocytes that seemed to migrate to the grafted zone. Interestingly, these keratinocytes strongly expressed the hyperproliferative keratin K6 (Fig. 7C,E, right panel). They also highly expressed CDSN, confirming that they originated from nude epidermis (data not shown). Hence, *Cdsn* deficiency resulted in chronic ulceration of the grafted skin. To study potential barrier defects at the level of the graft, TEWL measurements were performed. Values measured from 4 to 9 weeks post grafting ranged from 1.5 to 5 g m^{-2} per hour for the WT grafts versus 11.5 to 22.5 g m^{-2} per hour for the KO grafts, suggesting a strong permeability defect. Histological and immunohistological data suggested that the KO graft first behaved like a healing epidermis. However, whereas wound healing leads to barrier restoration and a return of keratinocytes to a normal differentiation program, the KO graft was unable to produce an efficient barrier. However, the epidermis of nude mice at the border of the scab showed acanthosis and perfectly mimicked a healing epidermis.

CDSN is also required in adult mice for epidermis integrity and barrier function

To investigate the consequences of CDSN loss in adult mice, we developed an additional model using a *K14*-promoter driven $CreER^{T2}$ recombinase, the activity of which is efficiently induced by 4-hydroxy-tamoxifen (OHT), but not natural estrogen receptor ligands (Li et al., 2000). Mice homozygous for the floxed *Cdsn* allele and transgenic for $K14CreER^{T2tg/0}$ were generated following the same breeding protocol described previously. Resulting animals were wild-type mice ($K14CreER^{T20/0}$:$Cdsn^{wt/fl}$ or $K14CreER^{T20/0}$:$Cdsn^{fl/fl}$), heterozygous pre-mutant mice ($K14CreER^{T2tg/0}$:$Cdsn^{wt/fl}$) and homozygous pre-mutant mice ($K14CreER^{T2tg/0}$:$Cdsn^{fl/fl}$, denoted hereafter HOMO). In the absence of treatment, HOMO mice did not develop any skin or hair phenotype for at least 6 months, denoting no leakiness of uninduced $CreER^{T2}$. Generalized or localized temporally controlled *Cdsn* excision was achieved in the skin of adult HOMO mice by intraperitoneal injection of tamoxifen (Tam) or topical application of OHT, respectively. In both cases, immunodetection of CDSN revealed a loss of *Cdsn* expression in epidermal keratinocytes and in the IRS of hair follicles (Fig. 8C; Fig. 9C). HOMO mice injected with Tam or locally treated with OHT developed a skin phenotype with variable kinetics according to the individuals but, once the phenotype had initiated, it progressed within 5 days to a critical situation. Wild-type mice treated in the same conditions never developed any phenotype, denoting the absence of toxicity of Tam or OHT in our experimental conditions. We attributed the variation in the kinetic of the HOMO mice phenotype onset to the genetic background heterogeneity of the mice. For this reason, we used TEWL values to evaluate the onset and progress of the phenotype.

Typically, TEWL values reached 4-5 g m^{-2} per hour when the first scales became visible, and rose to 33 g m^{-2} per hour as the scales became more numerous and were shed. After generalized induction of *Cdsn* deletion, the scales were first visible on the ventral side and snout, and then extended to the back and the whole body, consistent with the level of mechanical stress applied to these different body areas. Within 5 days of the abnormal skin phenotype onset, mice became prostrate, lost weight and were euthanized. A representative aspect of a ventral skin region with a TEWL value of 13 g m^{-2} per hour is presented in Fig. 8. At the histological level, acanthosis, hyperkeratosis and parakeratosis of the epidermis accompanied scaling (Fig. 8A,B,D, left panel). Topical applications of OHT were made, with the aim of analyzing the phenotype for a longer period of time (Fig. 9). Skin phenotype progression is presented at early (Fig. 9, middle panels) or late (Fig. 9, right panels) stages in comparison with the control (Fig. 9, left panels). The early stage showed a moderate barrier defect (TEWL of 11 g m^{-2} per hour) associated with the development of acanthosis, hyperkeratosis and parakeratosis, together with a strong expression of the hyperproliferative keratin K6 (Fig. 9, middle panel). At the late

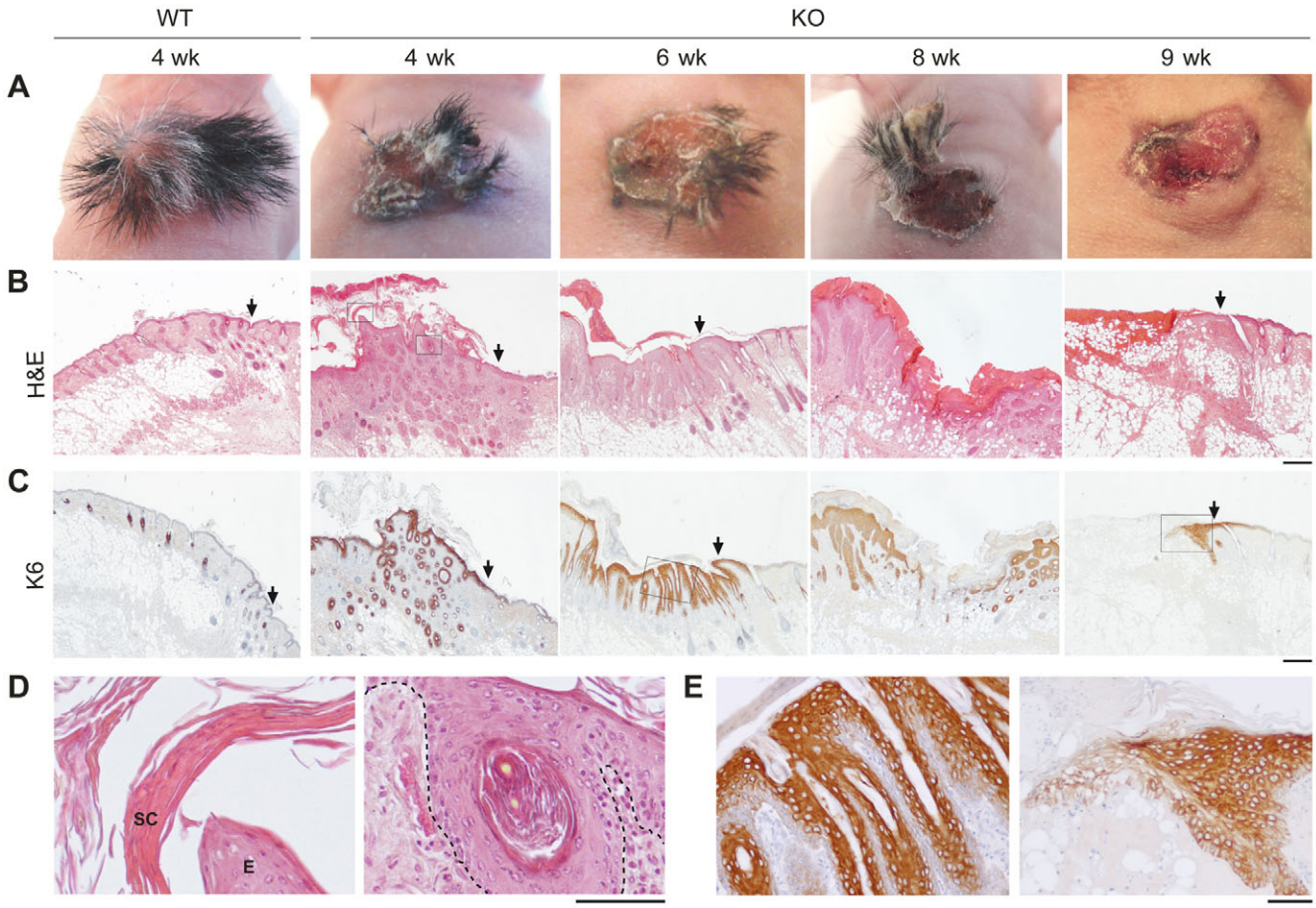

Fig. 7. Transplantation of *Cdsn*-deficient skin onto nude mice. Dorsal skin from WT or KO neonates was grafted onto the back of nude mice. Four weeks after grafting is shown as a representative stage for the WT graft, whereas 4, 6, 8 and 9 weeks after grafting are shown for the KO graft. (A) Macroscopic appearance of the transplanted skin. Grafts from KO mice develop few hairs, which become rarer and finally disappear. The skin is red, forms a scab and looks like a chronic healing area. Sections of WT or KO skin grafted onto nude mice were stained with hematoxylin and eosin (H&E) (B) or processed for immunohistochemistry with an antibody specific to K6 (C). Morphology of the grafted skin from WT mice is similar to that of adult mice skin. From 4 to 8 weeks, the KO grafted epidermis becomes acanthotic and develops prominent papillomatosis. The increasing K6 expression in epidermal keratinocytes confirms its hyperproliferative state. The KO grafted epidermis also develops prominent hyperkeratosis and parakeratosis. In the KO grafted skin, hair follicles become cystic then progressively disappear. They are totally absent by 9 weeks after grafting. Inflammatory infiltrate in the dermis from KO skin is obvious by 4 weeks after grafting, and diminishes in the course of the following weeks. Nine weeks after grafting, only a scab persists at the place of the KO grafted skin. K6 is only detected at the border of the graft, where the epidermis of the nude mice is thicker, denoting its hyperproliferative state. In B and C, the graft border is indicated with a vertical arrow. (D) Histological higher magnifications corresponding to the areas boxed in B show hyperkeratosis and parakeratosis (left) and dermal cyst formation (right). (E) Higher magnifications of skin sections after immunostaining with K6, corresponding to areas boxed in C, show hyperproliferative region (left) and edge of the KO graft (right). SC, stratum corneum; E, epidermis. Scale bars: 100 µm (B,C), 50 µm (D,E).

stage, corresponding to a TEWL value of 33 g m^{-2} per hour, ulcerations appeared and were associated with the shedding of large scales; histological analysis revealed almost complete disappearance of the epidermis, replaced by a scab (Fig. 9, right panel). At the early stages, moderate inflammation was observed, which we further characterized by immunohistochemistry for CD3 and F4/80 (supplementary material Fig. S1). It mainly consisted of $CD3^+$ T cells infiltrating the epidermis (supplementary material Fig. S1A) and macrophages and Langerhans cells in the dermis, at proximity of the epidermis (supplementary material Fig. S1B). The increasing barrier defect led to a typical inflammatory response, with ulceration, dilation of capillaries and subcorneal abscesses with neutrophils (see Fig. 9B, right panel).

Localized temporally controlled *Cdsn* excision in adult mouse skin also induced a notable morphological modification of the hair follicles. At early stages, they appeared to be distended and associated with hypertrophic sebaceous glands (Fig. 9B, middle panel). This was also the case when generalized *Cdsn* excision was induced (Fig. 8D). At later stages, hair follicles disappeared, as evidenced by the absence of K6 labeling (Fig. 9B,D, right panel). These observations are reminiscent of the neonatal-skin-grafted model, which is characterized by cyst formation and hair-follicle degeneration.

Discussion

In this study, we performed conditional ablation of *Cdsn* in mouse skin using *K14*-promoter driven Cre-mediated *loxP* recombination. Our results demonstrated that CDSN is necessary for epidermis integrity and barrier function in adult and neonatal mouse skin. *Cdsn* is also excised in the IRS of the hair follicles. At birth, hair follicles from KO mice appeared normal. However, they degenerated in KO

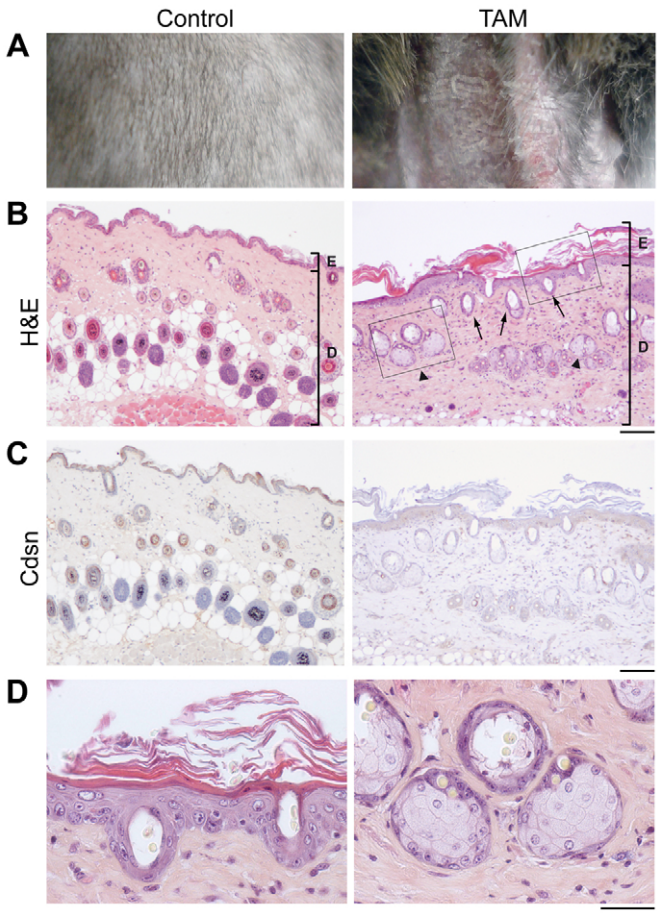

Fig. 8. Phenotype of generalized temporally controlled *Cdsn* KO in adult mouse skin. Shaved adult HOMO mice were injected with vehicle only (control) or with Tam (TAM) for 5 consecutive days, and checked daily for phenotype onset by clinical observation and TEWL measurement. (A) Macroscopic appearance of the mice. The ventral skin of the control mouse has no phenotype, whereas scales are visible on the ventral area of the TAM mouse. (B) Representative skin sections from ventral areas of control and TAM mice were stained with hematoxylin and eosin (H&E), showing acanthosis, hyperkeratosis and parakeratosis of the TAM mouse epidermis. In the dermis of TAM mouse, the hair follicles display an altered morphology; their upper part from the infudibulum to the skin surface is distended (arrows), and they are associated with hypertrophic sebaceous glands (arrowheads). D, dermis; E, epidermis. (C) Immunohistochemical staining with F28-27 mAb (CDSN) of ventral skin sections from control and TAM mice shows an effective loss of CDSN expression in the stratum granulosum of the epidermis and the IRS of the hair follicles in TAM mouse. (D) Higher magnification corresponding to the areas boxed in B shows in detail hyperproliferation, hyperkeratosis and abnormally distended hair follicles (left panel), hypertrophic sebaceous glands (right panel). Scale bars: 100 μm (B,C), 20 μm (D).

grafted skin as well as in the adult KO models, revealing that CDSN is also required for hair-follicle integrity.

Cdsn inactivation is useful to examine the function of CDSN within the corneodesmosome. As previously shown (Matsumoto et al., 2008), the major consequence observed here was an epidermal tear at sites of trauma and friction. Our detailed analysis of the neonatal phenotype showed that, although the greatly reduced mechanical resistance of the stratum corneum is an intrinsic feature caused by *Cdsn* deficiency, epidermal tear, leading to lethal barrier defect, occurred only under mechanical stress encountered after birth. At the histological level, blisters were found as soon as cornification occurred, that is, at the stratum granulosum to stratum corneum transition. Ultrastructural analysis revealed numerous split junctions with the main structure remaining attached to the granular keratinocytes, suggesting that the cohesive defect lies in the upper side of the junction. Thus, although CDSN is already present in the extracellular core of desmosomes from the stratum granulosum, it seems to have a fundamental role only when cornification is complete. Intriguingly, we did not observe thinning of single or bundled corneocytes throughout the stratum corneum, but detachment of the whole stratum corneum from the subjacent stratum granulosum. The stratum granulosum to stratum corneum interface might actually be the most fragile zone because it links two epidermal layers with different junctional organizations and mechanical characteristics: desmosomes and keratin intermediate filaments that are organized in taut cables in the stratum granulosum and rigid cornified envelopes linked by corneodesmosomes in the stratum corneum.

The underlying molecular mechanism by which CDSN assumes its adhesive function within the corneodesmosome has not been fully elucidated. In vivo, CDSN is known to be covalently linked to the cornified envelope (Serre et al., 1991). On the one hand, the previously demonstrated homophilic adhesive properties of CDSN and the strong resistance of aggregates formed by bacterially recombinant CDSN to highly denaturing conditions (Jonca et al., 2002; Caubet et al., 2004) suggest that, in vivo, CDSN reinforces cohesion by its own adhesive properties. On the other hand, adhesion provided by glycine-loop domains has been suggested to mediate reversible and constantly adjustable intermolecular links similar to Velcro (Steinert et al., 1991). Consistent with this, CDSN could give the junction the elasticity essential to prevent breaking as soon as the cell envelope rigidifies. Unlike the recent *Cdsn* inactivation study (Matsumoto et al., 2008), our ultrastructural analysis did not show any significant differences in the number of transitional desmosomes between WT and KO neonates. Moreover, the electron density of the corneodesmosomes appeared unchanged (Fig. 5). Thus, CDSN does not seem indispensable for the morphogenesis of corneodesmosomes, but appears essential to their function as adhesive structures.

Our *Cdsn* KO mice developed a phenotype that was very close to that displayed by *Spink5*$^{-/-}$ mice deficient for the serine protease inhibitor LektI. These mice exhibited fragile stratum corneum and perinatal death due to dehydration, with detachment of the stratum corneum from the subjacent epidermis layers and split desmosomes (Yang et al., 2004; Descargues et al., 2005). It was proposed that, in the absence of LektI, the premature proteolysis of CDSN or Dsg1 contributed significantly to desmosomal fragility, epidermal detachment and skin-barrier defects. It is interesting to note that, in both models, the breaking points mainly lie in the junction between living and cornified layers. This emphasizes the importance of corneodesmosomes as cornification takes place. However, the timing of the barrier defect differs between the two models: E18.5 for *Spink5*$^{-/-}$ mice but only after birth for our somatic *Cdsn*$^{-/-}$ mouse model. It is tempting to suggest that in the *Spink5*$^{-/-}$ model, the biochemical defect (absence of protease inhibitor) induces a dysfunction of the corneodesmosomes in utero, as soon as cornification occurs. By contrast, the absence of CDSN leads to a mechanical deficiency and thus the barrier impairment only takes place in the environment experienced after birth.

Grafting experiments demonstrated that the barrier defect extended postnatally. Skin from *Cdsn*-deficient grafts first developed acanthosis and hyperkeratosis. Increased expression of various

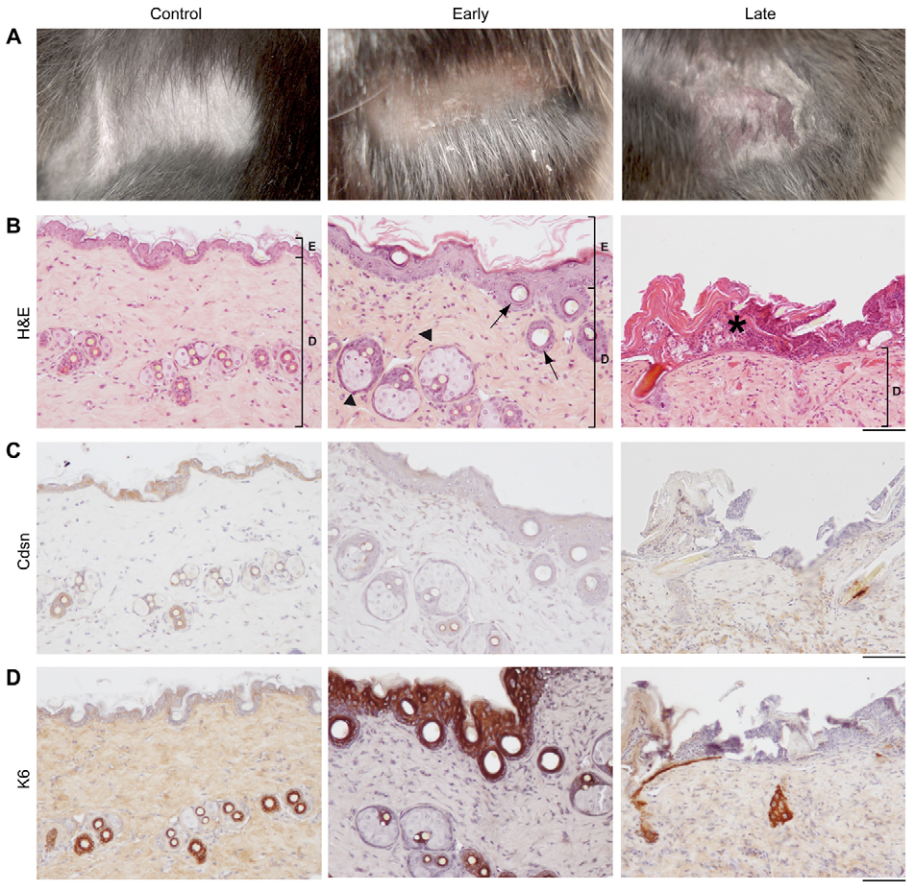

Fig. 9. Phenotype of localized temporally controlled *Cdsn* KO in adult mouse skin. Adult HOMO mice were shaved on both flanks and OHT was applied on the right flank for 5 consecutive days. The treated areas were checked daily for phenotype onset by clinical observation and TEWL measurement. (A) Macroscopic appearance of untreated left flank (control) or OHT-treated right flank from representative animals. Right flank of mice euthanized when the phenotype was moderate (early) or more severe (late), are presented. The scaling becomes more marked and ulceration of the skin appears as the phenotype progresses. (B) Representative skin sections from control, early or late flanks stained with hematoxylin and eosin (H&E). At early stage (middle panel), note the development of acanthosis, hyperkeratosis and parakeratosis, as well as the altered morphology of the hair follicles, which are distended from the infudibulum to the skin surface (arrows) and associated with hypertrophic sebaceous glands (arrowheads). At the late stage (right panel), hair follicles are no longer visible and a scab replaces the epidermis (asterisk). D, dermis; E, epidermis. (C,D) Skin sections from control, early or late flanks processed for immunohistochemical staining with F28-27 mAb (CDSN) (C) or with an antibody specific to K6 (D). Absence of labeling in early and late flanks confirms the efficient *Cdsn* excision in HOMO mouse skin treated with OHT, and the strong K6 expression confirms the hyperproliferative state of the HOMO mice epidermis. Scale bars: 50 μm.

differentiation markers (involucrin, K10), and induced expression of K6, confirmed the altered differentiation and the hyperproliferative state of the grafted epidermis. Hyperproliferation and acanthosis are thought to be compensatory responses to impaired epidermal barrier (Proksch et al., 1991). In the case of our *Cdsn*-deficient graft, these compensatory mechanisms appeared to be ineffective, and were followed by a complete disappearance of the epidermis. This demonstrates that CDSN is necessary for maintaining the integrity and barrier function of the postnatal epidermis. In our inducible models, the epidermal phenotype was very similar to that of our *Cdsn* KO skin graft model, although it progressed faster (within days). This might be due to the different location of the zone of interest, the interscapular area in the case of the grafts, and the flank in the inducible model, which is subjected to higher mechanical stress. Finally, in our inducible *Cdsn* KO models, barrier restoration remained unsuccessful, compromising the vital prognosis of the mice when the whole skin area was affected. Thus, CDSN seems to have a vital role in adult epidermis too.

Acanthosis, hyperkeratosis and parakeratosis are histological features more generally encountered in inflammatory epidermis, such as during wound healing or in psoriatic lesions. Although wound healing is transitory and rapidly leads to orthokeratotic epidermis and barrier repair, psoriatic epidermis maintains acanthosis, hyperkeratosis and parakeratosis with barrier defect. The situation has been described as a chronically persistent epidermal-healing state (Nickoloff et al., 2006). Our model of induction of *Cdsn* KO in adult mouse showed a persistent barrier defect similar to that observed in psoriasis. However, although we observed acanthosis, hyperkeratosis and parakeratosis at early stages, there was no formation of prominent and elongated rete ridges, only a weak inflammatory cell infiltrate, and the phenotype evolved towards ulceration and disappearance of the epidermis. In psoriasis, the barrier defect is thought to be associated with intrinsic immunological defects. The lack of any distinctive feature at the immunological level in our inducible KO model might contribute to the differences in the intensity of the inflammatory response. Finally, unlike our *Cdsn*-deficient mouse models, psoriasis is characterized by a significant increase in CDSN expression which is observed in multiple living layers and stratum corneum from lesional psoriatic epidermis (Haftek et al., 1997; Allen et al., 2001). However, the psoriasis-associated SNPs of *CDSN* could affect the function of the corresponding proteins, thus participating in the development of hyperproliferation as a compensatory mechanism to the barrier impairment. Assessment of the functional consequence of the amino acid substitution in alleles unique to risk haplotypes is needed to further investigate the putative involvement of CDSN in psoriasis pathophysiology.

Spatially controlled somatic *Cdsn* inactivation in mouse epidermis, using *K14*-promoter driven Cre-mediated deletion, also allowed inactivation of *Cdsn* in the developing hair follicle. Mice heterozygous for the excised *Cdsn* allele were indistinguishable from their wild-type littermates. In particular, they did not develop any hair phenotype up to 8 months. This suggests that the rare autosomal dominant human disease HSS is not caused by *Cdsn* haploinsufficiency. Moreover, recent work demonstrated that truncated CDSN, which accumulates abnormally as high-order

assemblies in the dermis of patients, organizes into proto-fibrillar structures in vitro and is toxic to keratinocytes (Cécile Caubet, Luc Bousset and G.S. et al., unpublished). Common features between CDSN mutant aggregates and amyloid deposits support HSS as a new potential amyloid disease and allow a better understanding of the HSS pathophysiology. Analysis of skin sections from newborn *Cdsn* KO mice showed a similar morphology and number of hair follicle to those in skin from WT littermates. The KO neonates also displayed normal whiskers. The only difference was that, in KO pup skin, no hair follicles expressed CDSN in the IRS. Therefore, CDSN seems to be dispensable for hair-follicle morphogenesis, as was the case for barrier establishment in the absence of external stress. The progressive degeneration of hair follicles and the formation of cysts observed from 4 weeks after grafting, together with the altered morphology and disappearance of hair follicles in adult mouse skin induced for *Cdsn* excision, suggest that CDSN is necessary for normal hair-follicle integrity. Mutation of another gene encoding a structural protein of the IRS, *DSG4*, is responsible for localized autosomal recessive hypotrichosis (LAH; OMIM 607903) (Kljuic et al., 2003). LAH is allelic with the lanceolate hair (lah) mouse, which fails to grow any normal hair and completely lacks vibrissae. Finally, the inactivation of genes encoding other desmosomal cadherins also leads to hair-follicle abnormalities. Mice deficient for Dsg3 or Dsc3, normally detected in the outer root sheath of the hair follicle, suffer from acantholysis between the two cell layers surrounding the telogen hair club, leading to telogen hair loss (Koch et al., 1998; Chen et al., 2008). Absence of Dsc1 in the IRS of hair follicles from *Dsc1*$^{-/-}$ mice induces localized hair loss associated with formation of utricali and dermal cysts denoting hair-follicle degeneration (Chidgey et al., 2001). Altogether, these data emphasize the importance of desmosomes and corneodesmosomes in hair-follicle integrity. In our different models, the hyperproliferative and inflammatory environment could aggravate the hair-follicle phenotype. A mouse model with specific inactivation of *Cdsn* in the IRS would be useful for an in-depth study of the consequences of *Cdsn* deletion on hair-follicle integrity.

Materials and Methods

Mice, tamoxifen treatment and skin grafting

Animals were handled according to the institutional guidelines and policies. The *Cdsn* mutant mouse line was established at the MCI/ICS (Mouse Clinical Institute/Institut Clinique de la Souris, Illkirch, France; http://www-mci.u-strasbg.fr). The targeting vector was constructed as follows. A 3 kb fragment encompassing most of the coding region (exon 2) and corresponding to the floxed region was amplified by PCR (from 129S2/SvPas genomic DNA) and subcloned in an MCI proprietary vector, resulting in step1 plasmid. The 5′ (4.7 kb) and the 3′ (3.5 kb) homologous arms were subcloned successively into the step 1 plasmid to generate the final targeting vector. All the coding regions were sequenced. The MCI vector has a flipped neomycin-resistance cassette. The linearized construct was electroporated in 129S2/SvPas mouse embryonic stem (ES) cells. After selection, targeted clones were identified by PCR using external primers and further confirmed by Southern blot with both Neo and 5′ external probes. One positive ES clone was injected into C57BL/6J blastocysts, and derived male chimeras gave germline transmission. Chimeric offspring were mated to FLPer (flipper) mice that express the Flp recombinase to excise the neomycin selection marker that was flanked by Frt sites. *K14-Cre* and *K14-CreER*^{T2} were described (Indra et al., 1999; Li et al., 2001). All experiments were performed on isolated mice. Tamoxifen (Tam) and 4-hydroxy-tamoxifen (OHT) (Sigma) were prepared as previously described (Indra et al., 1999). For *K14-CreER*^{T2} transgene activation, 8- to 10-week-old transgenic mice were either intraperitoneally injected with Tam (0.1 mg in 100 μl sunflower oil), or subjected to topical application of OHT (0.02 mg in 50 μl ethanol) on the shaved flank, for five consecutive days. For skin grafting, the dorsal skin harvested from KO (n=12) or WT (n=9) pups was grafted onto the back (interscapular region) of 7- to 8-week-old Rj:NMRI nude mice (Janvier, France) using the skin-flap technique (Barrandon et al., 1988). We removed the flap 2 weeks after grafting to bring the graft into an aerial environment, and started analysis 2 weeks later.

Primary antibodies

Rabbit polyclonal antibodies against K10, K6, filaggrin, involucrin, loricrin (all from Covance Research Products), Dsg1 (Santa Cruz Biotechnology), mouse mAb MAB1501 against actin (Chemicon International), rat mAb against CD3 (clone CD3-12, Serotec) and rat mAb against F4/80 (clone BM8, Serotec), were diluted following the manufacturers' recommendations. Mouse mAb F28-27, raised against human CDSN, crossreacting with mouse CDSN, was used as previously described (Serre et al., 1991).

Epidermal protein extraction and western blot analysis

Frozen tissues were homogenized in extraction buffer (40 mM Tris-HCl, 10 mM EDTA, 8 M urea, 0.25 mM PMSF, pH 7.4) with 0.1% v/v protease inhibitor cocktail (Sigma) by the FastPrep system (MP Biomedicals). Equal quantities of protein were separated by 12.5% SDS-PAGE and transferred to nitrocellulose membrane. The blots were probed with primary antibodies and HRP-conjugated secondary antibodies (Invitrogen). Detection was performed with ECL reagent (Amersham Pharmacia Biotech).

Histological and immunohistological analysis

Tissue samples were fixed for 24 hours in Bouin's fixative, dehydrated for 24 hours in 70% ethanol and embedded in paraffin. Sections (4 μm) were stained with hematoxylin and eosin or processed for immunohistochemical analysis. Rabbit polyclonal antibodies were detected with the appropriate ImmPRESS anti-rabbit Ig (peroxidase) kit whereas the Vector MOM peroxidase kit was used to detect CDSN (Vector Laboratories). Images were taken using a Nikon eclipse 80i microscope equipped with a Nikon DXM 1200C digital camera and NIS image analysis software.

Quantitative real-time PCR experiments

Skin samples were frozen immediately after dissection and total RNAs were isolated according to RNeasy mini columns protocol (Qiagen). Reverse transcription was performed using a combination of oligo(dT) and random hexamers. Primer sequences (supplementary material Table S1) were designed using Primer3 software to generate amplicons of 100-250 bp encompassing different exons. BLAST analysis (Altschul et al., 1997) ensured the absence of similarity to any other mouse sequence. Amplification assays were performed with the 7300 Real Time PCR System (Applied Biosystems) using the Sybr qPCR SuperMix with ROX (Invitrogen). Fluorescence was quantified as C_t (threshold cycle) values. Samples were analyzed in triplicate, with differences between the three C_t values lower than 0.3. Relative levels of gene expression between samples were determined using $2^{(-\Delta\Delta C_t)}$ (Livak and Schmittgen, 2001) with desmoglein 3 gene (*Dsg3*) expression for normalization. Control wells (without template cDNA) emitted no significant fluorescence. Specificity was assessed by sequencing the qRT-PCR amplicons.

Skin-barrier function assays

TEWL was measured using an EP1 Evaporimeter (Servo Med, AB Stockholm, Sweden). The dye exclusion assay was performed as previously described (Hardman et al., 1998; Marshall et al., 2000). The mice were then photographed using a Sony DSC-W50 camera. For quantification of stratum corneum removal by tape stripping, a quarter of a D-Squame disk (22 mm diameter, Monaderm) was placed on the flank of neonates and stripped off, and the process was repeated once on the same area. Tape disc fragments were incubated with shaking in 250 μl extraction buffer (40 mM Tris-HCl, 10 mM EDTA, 8 M urea, 50 mM dithiothreitol, pH 7.4) for 1 hour at 70°C, then centrifuged for 5 minutes at 12,000 r.p.m. and the protein content was measured in the supernatant using a colorimetric protein assay (Bio-Rad).

Transmission electron microscopy

Specimens were fixed for at least 4 hours in 2% glutaraldehyde in Sorensen's buffer (pH 7.4), washed with Sorensen's buffer, cut into pieces of ~1 mm^3, postfixed for 1 hour at room temperature in 1% osmium, 250 mM saccharose in Sorensen's buffer (pH 7.4), dehydrated through graded ethanol solutions, transferred into propylene oxide and embedded in araldite resin. Ultrathin 90 nm sections cut on a Reichert Ultracut ultramicrotome were stained with uranyle acetate and lead citrate and examined with an electron microscope (Hitachi HU12A).

The floxed mouse mutant line was established at the Mouse Clinical Institute (Institut Clinique de la Souris, MCI/ICS) in the Targeted Mutagenesis and Transgenesis Department with funds from the GIS-Institut des Maladies Rares. The authors would like to thank H. Gallinaro for participating in the targeting strategy, and M. Ribouchon for excellent technical assistance. We thank staff of INSERM-IFR150, and more particularly M. Calise, S. Appolinaire, A. Tridon, P. Aregui, G. Marsal from the animal facilities, F. Capilla and T. Al Saati from the technical platform of 'histopathologie expérimentale', C. Offer and H. Brun from the 'plateau de séquençage'. We also thank I. Fourquaux from the CMEAB for technical assistance with ultrastructural analysis. This study was supported by grants from the CNRS, Toulouse III University, the 'Société de Recherche Dermatologique' (SRD) and the 'Association Alopecia Areata' (AAA).

References

Allen, M., Ishida-Yamamoto, A., McGrath, J., Davison, S., Iizuka, H., Simon, M., Guerrin, M., Hayday, A., Vaughan, R., Serre, G. et al. (2001). Corneodesmosin expression in psoriasis vulgaris differs from normal skin and other inflammatory skin disorders. *Lab. Invest.* **81**, 969-976.

Altschul, S. F., Madden, T. L., Schaffer, A. A., Zhang, J., Zhang, Z., Miller, W. and Lipman, D. J. (1997). Gapped BLAST and PSI-BLAST: a new generation of protein database search programs. *Nucleic Acids Res.* **25**, 3389-3402.

Barrandon, Y., Li, V. and Green, H. (1988). New techniques for the grafting of cultured human epidermal cells onto athymic animals. *J. Invest. Dermatol.* **91**, 315-318.

Capon, F., Munro, M., Barker, J. and Trembath, R. (2002). Searching for the major histocompatibility complex psoriasis susceptibility gene. *J. Invest. Dermatol.* **118**, 745-751.

Capon, F., Toal, I. K., Evans, J. C., Allen, M. H., Patel, S., Tillman, D., Burden, D., Barker, J. N. and Trembath, R. C. (2003). Haplotype analysis of distantly related populations implicates corneodesmosin in psoriasis susceptibility. *J. Med. Genet.* **40**, 447-452.

Caubet, C., Jonca, N., Lopez, F., Estève, J. P., Simon, M. and Serre, G. (2004). Homo-oligomerization of human corneodesmosin is mediated by its N-terminal glycine loop domain. *J. Invest. Dermatol.* **122**, 747-754.

Chen, J., Den, Z. and Koch, P. J. (2008). Loss of desmocollin 3 in mice leads to epidermal blistering. *J. Cell Sci.* **121**, 2844-2849.

Chidgey, M., Brakebusch, C., Gustafsson, E., Cruchley, A., Hail, C., Kirk, S., Merritt, A., North, A., Tselepis, C., Hewitt, J. et al. (2001). Mice lacking desmocollin 1 show epidermal fragility accompanied by barrier defects and abnormal differentiation. *J. Cell Biol.* **155**, 821-832.

Descargues, P., Deraison, C., Bonnart, C., Kreft, M., Kishibe, M., Ishida-Yamamoto, A., Elias, P., Barrandon, Y., Zambruno, G., Sonnenberg, A. et al. (2005). Spink5-deficient mice mimic Netherton syndrome through degradation of desmoglein 1 by epidermal protease hyperactivity. *Nat. Genet.* **37**, 56-65.

Garrod, D. and Chidgey, M. (2008). Desmosome structure, composition and function. *Biochim. Biophys. Acta* **1778**, 572-587.

Guerrin, M., Simon, M., Montézin, M., Haftek, M., Vincent, C. and Serre, G. (1998). Expression cloning of human corneodesmosin proves its identity with the product of the S gene and allows improved characterization of its processing during keratinocyte differentiation. *J. Biol. Chem.* **273**, 22640-22647.

Haftek, M., Simon, M., Kanitakis, J., Maréchal, S., Claudy, A., Serre, G. and Schmitt, D. (1997). Expression of corneodesmosin in the granular layer and stratum corneum of normal and diseased epidermis. *Br. J. Dermatol.* **137**, 864-873.

Hardman, M. J., Sisi, P., Banbury, D. N. and Byrne, C. (1998). Patterned acquisition of skin barrier function during development. *Development* **125**, 1541-1552.

Helms, C., Saccone, N. L., Cao, L., Daw, J. A., Cao, K., Hsu, T. M., Taillon-Miller, P., Duan, S., Gordon, D., Pierce, B. et al. (2005). Localization of PSORS1 to a haplotype block harboring HLA-C and distinct from corneodesmosin and HCR. *Hum. Genet.* **118**, 466-476.

Indra, A. K., Warot, X., Brocard, J., Bornert, J. M., Xiao, J. H., Chambon, P. and Metzger, D. (1999). Temporally-controlled site-specific mutagenesis in the basal layer of the epidermis: comparison of the recombinase activity of the tamoxifen-inducible Cre-ER(T) and Cre-ER(T2) recombinases. *Nucleic Acids Res.* **27**, 4324-4327.

Jonca, N., Guerrin, M., Hadjiolova, K., Caubet, C., Gallinaro, H., Simon, M. and Serre, G. (2002). Corneodesmosin, a component of epidermal corneocyte desmosomes, displays homophilic adhesive properties. *J. Biol. Chem.* **277**, 5024-5029.

Kljuic, A., Bazzi, H., Sundberg, J. P., Martinez-Mir, A., O'Shaughnessy, R., Mahoney, M. G., Levy, M., Montagutelli, X., Ahmad, W., Aita, V. M. et al. (2003). Desmoglein 4 in hair follicle differentiation and epidermal adhesion: evidence from inherited hypotrichosis and acquired pemphigus vulgaris. *Cell* **113**, 249-260.

Koch, P. J., Mahoney, M. G., Cotsarelis, G., Rothenberger, K., Lavker, R. M. and Stanley, J. R. (1998). Desmoglein 3 anchors telogen hair in the follicle. *J. Cell Sci.* **111**, 2529-2537.

Kottke, M. D., Delva, E. and Kowalczyk, A. P. (2006). The desmosome: cell science lessons from human diseases. *J. Cell Sci.* **119**, 797-806.

Lai-Cheong, J. E., Arita, K. and McGrath, J. A. (2007). Genetic diseases of junctions. *J. Invest. Dermatol.* **127**, 2713-2725.

Levy-Nissenbaum, E., Betz, R. C., Frydman, M., Simon, M., Lahat, H., Bakhan, T., Goldman, B., Bygum, A., Pierick, M., Hillmer, A. M. et al. (2003). Hypotrichosis simplex of the scalp is associated with nonsense mutations in CDSN encoding corneodesmosin. *Nat. Genet.* **34**, 151-153.

Li, M., Indra, A. K., Warot, X., Brocard, J., Messaddeq, N., Kato, S., Metzger, D. and Chambon, P. (2000). Skin abnormalities generated by temporally controlled RXRalpha mutations in mouse epidermis. *Nature* **407**, 633-636.

Li, M., Chiba, H., Warot, X., Messaddeq, N., Gérard, C., Chambon, P. and Metzger, D. (2001). RXR-alpha ablation in skin keratinocytes results in alopecia and epidermal alterations. *Development* **128**, 675-688.

Livak, K. J. and Schmittgen, T. D. (2001). Analysis of relative gene expression data using real-time quantitative PCR and the 2(-Delta Delta C(T)) Method. *Methods* **25**, 402-408.

Lundström, A., Serre, G., Haftek, M. and Egelrud, T. (1994). Evidence for a role of corneodesmosin, a protein which may serve to modify desmosomes during cornification, in stratum corneum cell cohesion and desquamation. *Arch. Dermatol. Res.* **286**, 369-375.

Marshall, D., Hardman, M. J. and Byrne, C. (2000). SPRR1 gene induction and barrier formation occur as coordinated moving fronts in terminally differentiating epithelia. *J. Invest. Dermatol.* **114**, 967-975.

Matsumoto, M., Zhou, Y., Matsuo, S., Nakanishi, H., Hirose, K., Oura, H., Arase, S., Ishida-Yamamoto, A., Bando, Y., Izumi, K. et al. (2008). Targeted deletion of the murine corneodesmosin gene delineates its essential role in skin and hair physiology. *Proc. Natl. Acad. Sci. USA* **105**, 6720-6724.

Nair, R. P., Stuart, P. E., Nistor, I., Hiremagalore, R., Chia, N. V., Jenisch, S., Weichenthal, M., Abecasis, G. R., Lim, H. W., Christophers, E. et al. (2006). Sequence and haplotype analysis supports HLA-C as the psoriasis susceptibility 1 gene. *Am. J. Hum. Genet.* **78**, 827-851.

Nickoloff, B. J., Bonish, B. K., Marble, D. J., Schriedel, K. A., DiPietro, L. A., Gordon, K. B. and Lingen, M. W. (2006). Lessons learned from psoriatic plaques concerning mechanisms of tissue repair, remodeling, and inflammation. *J. Investig. Dermatol. Symp. Proc.* **11**, 16-29.

Orrù, S., Giuressi, E., Carcassi, C., Casula, M. and Contu, L. (2005). Mapping of the major psoriasis-susceptibility locus (PSORS1) in a 70-Kb interval around the corneodesmosin gene (CDSN). *Am. J. Hum. Genet.* **76**, 164-171.

Proksch, E., Feingold, K. R., Man, M. Q. and Elias, P. M. (1991). Barrier function regulates epidermal DNA synthesis. *J. Clin. Invest.* **87**, 1668-1673.

Serre, G., Mils, V., Haftek, M., Vincent, C., Croute, F., Reano, A., Ouhayoun, J. P., Bettinger, S. and Soleilhavoup, J. P. (1991). Identification of late differentiation antigens of human cornified epithelia, expressed in re-organized desmosomes and bound to cross-linked envelope. *J. Invest. Dermatol.* **97**, 1061-1072.

Simon, M., Montézin, M., Guerrin, M., Durieux, J. J. and Serre, G. (1997). Characterization and purification of human corneodesmosin, an epidermal basic glycoprotein associated with corneocyte-specific modified desmosomes. *J. Biol. Chem.* **272**, 31770-31776.

Simon, M., Jonca, N., Guerrin, M., Haftek, M., Bernard, D., Caubet, C., Egelrud, T., Schmidt, R. and Serre, G. (2001). Refined characterization of corneodesmosin proteolysis during terminal differentiation of human epidermis and its relationship to desquamation. *J. Biol. Chem.* **276**, 20292-20299.

Steinert, P. M., Mack, J. W., Korge, B. P., Gan, S. Q., Haynes, S. R. and Steven, A. C. (1991). Glycine loops in proteins: their occurrence in certain intermediate filament chains, loricrins and single-stranded RNA binding proteins. *Int. J. Biol. Macromol.* **13**, 130-139.

Vassar, R., Rosenberg, M., Ross, S., Tyner, A. and Fuchs, E. (1989). Tissue-specific and differentiation-specific expression of a human K14 keratin gene in transgenic mice. *Proc. Natl. Acad. Sci. USA* **86**, 1563-1567.

Veal, C. D., Capon, F., Allen, M. H., Heath, E. K., Evans, J. C., Jones, A., Patel, S., Burden, D., Tillman, D., Barker, J. N. et al. (2002). Family-based analysis using a dense single-nucleotide polymorphism-based map defines genetic variation at PSORS1, the major psoriasis-susceptibility locus. *Am. J. Hum. Genet.* **71**, 554-564.

Wang, X., Zinkel, S., Polonsky, K. and Fuchs, E. (1997). Transgenic studies with a keratin promoter-driven growth hormone transgene: prospects for gene therapy. *Proc. Natl. Acad. Sci. USA* **94**, 219-226.

Yang, T., Liang, D., Koch, P. J., Hohl, D., Kheradmand, F. and Overbeek, P. A. (2004). Epidermal detachment, desmosomal dissociation, and destabilization of corneodesmosin in Spink5–/– mice. *Genes Dev.* **18**, 2354-2358.